[25] X. Pan, T. Terada, M. Okuda, K. Inui, Altered diurnal rhythm of intestinal peptide transporter by fasting and its effects on the pharmacokinetics of ceftibuten, J. Pharmacol. Exp. Ther. 307 (2003) 626–632.

[26] H. Ogihara, T. Suzuki, Y. Nagamachi, K. Inui, K. Takata, Peptide transporter in the rat small intestine: ultrastructural localization and the effect of starvation and administration of amino acids, Histochem. J. 31 (1999) 169–174.

[27] K. Izuishi, K. Kato, T. Ogura, T. Kinoshita, H. Esumi, Remarkable tolerance of tumor cells to nutrient deprivation: possible new biochemical target for cancer therapy, Cancer Res. 60 (2000) 6201–6207.

ELSEVIER

# Expression profiles of various transporters for oligopeptides, amino acids and organic ions along the human digestive tract

Tomohiro Terada[a], Yutaka Shimada[b], Xiaoyue Pan[a], Koshiro Kishimoto[a],
Takaki Sakurai[c], Ryuichiro Doi[b], Hisashi Onodera[b], Toshiya Katsura[a],
Masayuki Imamura[b], Ken-ichi Inui[a,*]

[a] Department of Pharmacy, Kyoto University Hospital, Sakyo-ku, Kyoto 606-8507, Japan
[b] Surgery and Surgical Basic Science, Graduate School of Medicine, Kyoto University, Japan
[c] Laboratory of Anatomic Pathology, Kyoto University Hospital, Japan

## Abstract

Various transporters such as $H^+$/peptide cotransporter PEPT1 are expressed in the intestine, and play important physiological and pharmacological roles in the body. Present study was performed to examine the expression profile of 20 kinds of transporters (PEPT1 and 2, P-glycoprotein, amino acid transporters and organic ion transporters) along the human digestive tract, especially focusing on PEPT1. Using normal mucosal specimens, real-time polymerase chain reactions were carried out. Immunoblot analyses were also performed for PEPT1 expression. PEPT1 mRNA was highly expressed in the small intestine (duodenum > jejunum > ileum) compared to other tissues, and some patients showed a significant level of expression in the stomach. The expressional pattern of PEPT1 in the stomach and histological diagnosis indicated that gastric PEPT1 originated from the intestinal metaplasia. The amino acid transporters showed unique mRNA expression levels and distributions in the digestive tract. For example, the expression levels of $B^0AT1$, a $Na^+$-dependent and chloride-independent neutral amino acid transporter, were increased from the duodenum to ileum, which pattern is completely inverted to that for PEPT1. There is little expression of organic ion transporters except for organic cation/carnitine transporter OCTN2. In conclusion, PEPT1 was abundantly expressed in the small intestine, and the reciprocal expression of PEPT1 and $B^0AT1$ may serve for the efficient absorption of protein digestive products.

## 1. Introduction

Cellular uptake of small peptides (di- and tri-peptides) is mediated by a $H^+$/peptide cotransporter at the brush-border membranes of intestinal absorptive epithelial cells [1,2]. Cloning studies have clarified the molecular nature of the intestinal $H^+$/peptide cotransporter (PEPT1) in various species [2,3]. Another $H^+$/peptide cotransporter, human PEPT2 is expressed mainly in the kidney, but not in the small intestine, and has a higher affinity for most substrates [3]. As PEPT1 has broad substrate specificity, the intestinal absorption of several pharmacologically active drugs, such as oral β-lactam antibiotics and the anti-viral agent vala-

cyclovir are mediated by this transporter, and therefore, PEPT1 also plays important roles as a drug transporter [3].

In addition to PEPT1, various amino acid transport systems, such as L, $y^+$, $y^+L$, $b^{0,+}$, A, ASC, $B^0$, $B^{0,+}$ and $X_{AG}^-$ are expressed in the small intestinal epithelial cells. These systems have been classified by their ion-dependence and substrate specificity [4], and the molecular nature of each system has been identified [5,6]. For example, system $B^0$, which is a $Na^+$-dependent and chloride-independent transporter, is responsible for the uptake of most neutral amino acids at the brush-border membranes of intestinal epithelial cells [7,8]. Two independent groups have recently isolated and characterized the transporter cDNA corresponding to system $B^0$ ($B^0AT1$), and demonstrated that a mutation of $B^0AT1$ results in the Hartnup disorder [9,10].

* Corresponding author. Tel.: +81 75 751 3577; fax: +81 75 751 4207.
  *E-mail address:* inui@kuhp.kyoto-u.ac.jp (K.-i. Inui).

Although the number of peptide transporters is smaller than that of amino acid transporters, numerous investigations have shown that the peptide transporters play a major role in the completion of the final step of protein digestion in the human intestine [1]. These findings led us to examine the expression levels of each transporter along the human digestive tract. Thus, in the present study, using normal portions of mucosal samples from cancer patients treated surgically, mRNA expression levels of PEPT1 and seven amino acid transporters were qualified by real-time PCR techniques. Furthermore, to investigate the pharmacokinetic aspects of PEPT1, we compared mRNA expression level of PEPT1 with those of other drug transporters, i.e., organic ion transporters. We previously examined the expression profiles of organic ion transporters in the kidney [11], but there is little information about their expression in the human gut.

## 2. Material and methods

### 2.1. Patients and tissue sampling

The mucosal samples from normal tissues along the digestive tract and normal pancreatic tissue were obtained from cancer patients during surgery at the First Department of Surgery, Kyoto University Hospital. Normal mucosal samples were resected at the site most distant from the affected portions. Table 1 shows the number, sex and age of patients for each tissue sample. No patients underwent preoperative chemotherapy and/or radiation therapy. The samples were frozen in liquid nitrogen and stored at −80 °C until RNA extraction and membrane preparation. This study was conducted in accordance with the Declaration of Helsinki and its amendments, and was approved by the Ethics Committee of Kyoto University (G-39). Written informed consent was obtained from all patients for surgery and use of their resected samples.

### 2.2. Isolation of total RNA

Total cellular RNA was isolated from the tissue samples using a MagNA Pure LC RNA isolation Kit II (Roche Diagnostic GmbH, Mannheim, Germany) according to the

Table 1
The number, sex and age of patients for each tissue sample

|  | n | Male | Female | Age (years) |
| --- | --- | --- | --- | --- |
| Esophagus | 16 | 13 | 3 | 59.3 ± 1.6 |
| Stomach | 31 | 20 | 11 | 64.4 ± 2.3 |
| Duodenum | 13 | 7 | 6 | 63.8 ± 2.2 |
| Jejunum | 15 | 13 | 2 | 66.6 ± 3.7 |
| Ileum | 10 | 4 | 6 | 65.3 ± 5.7 |
| Colon | 15 | 8 | 7 | 71.6 ± 3.1 |
| Rectum | 15 | 11 | 4 | 64.6 ± 3.0 |
| Pancreas | 9 | 3 | 6 | 61.8 ± 2.8 |

manufacturer's instructions, and the concentrations of total cellular RNA were measured by spectrophotometry. Isolated total RNA was reverse-transcribed and the reaction mixtures were used for real-time PCR.

### 2.3. Real-time PCR

Primers and probes for PEPT1 and 2, seven amino acid transporters and urate transproter (URAT1) were designed using the Primer Express® software program (Table 2). Those for multidrug resistance 1 (MDR1) [12] and organic ion transporters [11] were previously designed. Oligonucleotide probes were labelled with a fluorogenic dye, 6 carboxyfluorescein (Fam) and quenched with 6 carboxy-tetramethylrhodamine (Tamra) (Table 2). Real-time PCR was performed in an ABI PRISM 7700 (Applied Biosystems, Foster, CA) and quantification by use of standard plasmid DNA was performed as described previously [11]. For each reaction, the assay was carried out in duplicate. Glycerolaldehyde 3-phosphate denydrogenase (GAPDH) mRNA was also measured as an internal control with GAPDH control reagent (Applied Biosystems).

### 2.4. Antibodies

Rabbit anti-human PEPT1 antibody was prepared previously, and the specificity was already confirmed [13]. Mouse anti-$Na^+/K^+$-ATPase monoclonal antibody was purchased from Upstate Biotechnology (Lake Placid, NY). For immunohistochemistry, we used anti-CD10 antibody (Novocastra Laboratories Ltd., Newcastle upon Tyne, UK).

### 2.5. Western blot analysis

Crude plasma membranes were prepared from tissue samples taken along the digestive tract as described previously [11]. Western blot analyses using affinity-purified anti-PEPT1 antibody [13] and mouse monoclonal $Na^+/K^+$-ATPase antibody [11] were carried out based on our previous reports.

### 2.6. Immunohistochemistry

Paraffin-embeded sections were stained for CD10 antibody. The sections were deparaffinized, and antigens were retrieved by autoclave in 10 mM EDTA buffer (pH 8.0) for 15 min. Non-specific antigen was blocked by 10% normal horse serum for 30 min at room temperature. Anti-CD10 antibody (×50) in PBS containing 1% bovine serum albumin was applied and sections were incubated at 37 °C for 32 min. Slides were washed six times in PBS, and then incubated with biotinylated horse anti-mouse antibody for 40 min at room temperature. The slides were then counterstained with hematoxylin.

Table 2
Primer sets and probes used for real-time PCR

| | Sequence | Nucleotide numbers | Accession number |
|---|---|---|---|
| **PEPT1** | | | NM_005073 |
| Forward primer | attgtgtcgctctccattgtctac | 306–329 | |
| Reverse primer | atgacctcacagaccacaaccat | 389–367 | |
| TaqMan probe | ttggacaagcagtcacctcagtaagctcca | 334–363 | |
| **PEPT2** | | | NM_021082 |
| Forward primer | ttaaacaaggccccagagactct | 2382–2404 | |
| Reverse primer | cccacttagttctggacctgctt | 2463–2445 | |
| TaqMan probe | tgccccaaccagtcttcaggaggaag | 2410–2439 | |
| **B⁰AT1** | | | XM_291120 |
| Forward primer | gtgtggacaggttcaataaggacat | 1646–1670 | |
| Reverse primer | ccacgtgacttgccagaagat | 1719–1699 | |
| TaqMan probe | tcatgatcggccacaagcccaa | 1676–1697 | |
| **ASCT2** | | | U53347 |
| Forward primer | gcgagaaatatcttcccttcca | 1152–1202 | |
| Reverse primer | gttccggtgatattcctctcttca | 1266–1243 | |
| TaqMan probe | tgtcagcagcctttcgctcatactctacca | 1209–1238 | |
| **b⁰·⁺AT** | | | AF141289 |
| Forward primer | ggcctgacgattctaggactca | 1344–1365 | |
| Reverse primer | ggagccagaaccaaaaacaca | 1468–1448 | |
| TaqMan probe | atcaaggtgcccgtagtcattcccgt | 1404–1429 | |
| **LAT1** | | | AF104032 |
| Forward primer | ggaagacacccgtggagtgt | 1421–1440 | |
| Reverse primer | acaggacggtcgtggagaag | 1552–1533 | |
| TaqMan probe | tggaaaaacaagcccaagtggctcc | 1498–1522 | |
| **LAT2** | | | AF171669 |
| Forward primer | tgaggagcttgttgatccctaca | 988–1010 | |
| Reverse primer | gcgacattggcaaagacataca | 1080–1059 | |
| TaqMan probe | tcccagagccatcttcatctccatcc | 1018–1043 | |
| **y⁺LAT1** | | | AF092032 |
| Forward primer | gatccatgttgagcggttcac | 1336–1356 | |
| Reverse primer | ccacgcacaagtagatcaatgc | 1412–1391 | |
| TaqMan probe | ccagtgccttctctgctcttcaatggtatc | 1358–1387 | |
| **ATA2** | | | AF259799 |
| Forward primer | gacagcagcagctacagttcca | 66–87 | |
| Reverse primer | cataatggcttttcagagcagctt | 144–121 | |
| TaqMan probe | agcgacttcaactactcctaccccaccaag | 90–119 | |
| **URAT1** | | | AB071863 |
| Forward primer | agctcttggaccccaatgc | 437–455 | |
| Reverse primer | cttcagagcgtgagagtcacaca | 560–582 | |
| TaqMan probe | cgcagcatcttcacctccacaatcgt · | 517–542 | |

Primers and probes used for real-time PCR. All primers and probes were designed using Primer Express software from Applied Biosystems. Primers were tested using RT-PCR and only those yielding a single band of the expected size were used for subsequent real-time PCR experiments.

## 3. Results

### 3.1. Quantification of PEPT1 and PEPT2 mRNA in tissues along the digestive tract and pancreas

First, to verify the conditions and experimental techniques, MDR1 mRNA expression levels were measured (Fig. 1 right). We previously found that the level of MDR1 mRNA in the jejunum from living-donor liver transplantation patients was 0.41 ± 1.19 amol/μg of total RNA (mean ± S.E., $n = 48$) using a competitive PCR-based method, and that the level of MDR1 mRNA correlated well with protein level [14]. In the present study, the MDR1 mRNA level in the jejunum was 2.73 ± 0.51 amol/μg of total RNA (mean ± S.E., $n = 16$). This value was similar to previously reported ones [14]. Furthermore, MDR1 mRNA levels gradually increased from the duodenum to ileum, well consistent with previous findings on the distribution of MDR1 mRNA [15] and P-glycoprotein [16] in the human small intestine (Fig. 1 right). The expression of MDR1 mRNA in the colon and rectum (Fig. 1 right) also corresponded to a previous report [17]. All these findings suggested that the conditions and experimental techniques were reliable.

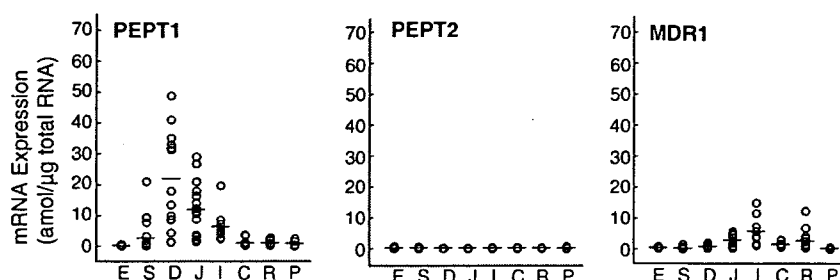We then examined the mRNA expression of PEPT1 and PEPT2 along the digestive tract (esophagus, stomach,

Fig. 1. mRNA expression of PEPT1, PEPT2 and MDR1 along the digestive tract (esophagus (E), stomach (S), duodenum (D), jejunum (J), ileum (I), colon (C), rectum (R)) and pancreas (P). Total cellular RNA was extracted from each tissue sample, and reverse-transcribed. The mRNA levels were determined by real-time PCR using an ABI prism 7700 sequence detector.

duodenum, jejunum, ileum, colon and rectum) and pancreas. As shown in Fig. 1 left, PEPT1 mRNA is highly expressed in the small intestine (duodenum > jejunum > ileum), but is not expressed or only slightly expressed in the esophagus, colon, rectum and pancreas. In the stomach, some patients showed a high level of PEPT1 mRNA. The tissue which showed the highest expression level was the duodenum (22.0 ± 4.23 amol/μg RNA). In contrast to PEPT1 mRNA, PEPT2 mRNA was not expressed in all tissues examined (Fig. 1 middle).

### 3.2. Western blot analysis

Fig. 2 shows Western blot analyses using crude membranes from each tissue. A primary band of about 80 kDa of PEPT1 protein was detected in the stomach, duodenum, jejunum and ileum, as observed in the mRNA analyses. In other tissues, no PEPT1 protein was detected. In the case of PEPT2 protein, there were no detectable bands in the tissue samples from along the digestive tracts (data not shown). The protein band of Na$^+$/K$^+$-ATPase was detected in all specimens (Fig. 2).

### 3.3. PEPT1 in the stomach

There is no expression of PEPT1 protein in the rat stomach [18]. On the other hand, the present study has demonstrated that some patients had a relatively high level of PEPT1 in the stomach, although there were interindividual differences. To clarify the distribution of PEPT1 in the gastric mucosa, fundus (the upper-third: U), body (the middle-third: M) and antrum (the lower-third: L) mucosa were assessed for PEPT1 protein expression when sections were available from one patient. As shown in Fig. 3,
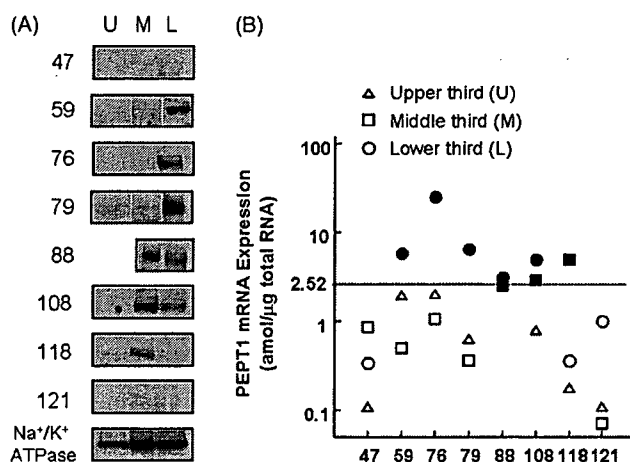


Fig. 3. PEPT1 expression in the gastric mucosa. (A) Crude membranes were isolated from the upper-third (U), middle-third (M) and lower-third (L) of the gastric mucosa from eight patients and subjected to Western blot analyses (50 μg protein/lane) for PEPT1 and Na$^+$/K$^+$-ATPase. Conditions for Western blotting were identical to those in Fig. 2. For Na$^+$/K$^+$-ATPase, representative data are shown. A sample for the upper-third of patient 88 was not obtained. (B) Relationship between mRNA and protein expression levels of PEPT1 in gastric mucosa. Closed symbols represent the samples with PEPT1 protein expression. When the mRNA level was more than 2.52 amol/μg of total RNA, the band for PEPT1 protein was detected.

PEPT1 protein was expressed in the antral mucosa in most cases, and well correlated with mRNA expression level. When the mRNA level was more than 2.52 amol/μg of total RNA, the band for PEPT1 protein was detected.

These expressional patterns and the histological diagnosis suggested that intestinal metaplasia may induce the expression of PEPT1 in the stomach. Intestinal metaplasia primarily affects the antrum in a patchy fashion, and the superficial gastric epithelium is replaced by intestinal goblet and absorptive cells [19]. Using paraffin sections
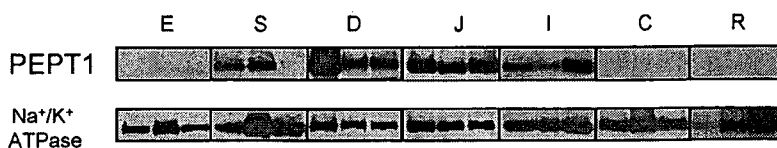


Fig. 2. Western blot analyses of crude membranes isolated from human tissues along the digestive tract for PEPT1 and Na$^+$/K$^+$ ATPase. Crude membranes were isolated from each tissue and subjected to Western blotting (50 μg protein/lane). Abbreviations for each tissue are identical to those in Fig. 1. PEPT1 protein was identified using affinity-purified anti-PEPT1 antibody (1:500 dilution). After the membranes were deprobed, Na$^+$/K$^+$-ATPase protein was detected by the mouse monoclonal anti Na$^+$/K$^+$-ATPase antibody (1:10,000).

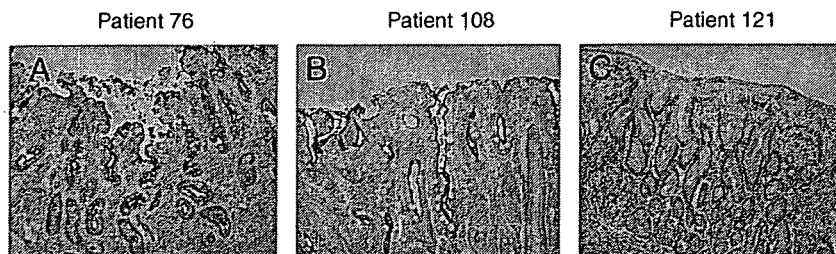Patient 76                    Patient 108                    Patient 121



Fig. 4. Localization of CD10 in the intestinal metaplasia. (A and B) CD10 can be seen along the brush-border membranes of the luminal surface of the epithelium in antral mucosa from patients 76 and 108 (original magnification ×50). (C) Hematoxilin–eosin staining of antral mucosa from patient 121.

of antral mucosa from patients 76, 108 and 121, immunostaining for CD10 was carried out. CD10, also known as enkephalinase, has been shown to localize to the brush-border membranes of absorptive small intestinal enterocytes [20]. CD10 was positively expressed along the luminal surface of the epithelium of patients 76 and 108 (Fig. 4A and B), but not patient 121 (data not shown). Hematoxilin–eosin staining revealed that intestinal metaplasia did not occurr in patient 121 (Fig. 4C).

### 3.4. Comparison of mRNA expression levels of PEPT1 with those of amino acid transporters in the digestive tract

We next examined the expression profile of amino acid transporters in the digestive tract to compare with PEPT1. The human amino acid transporters examined here were mainly neutral amino acid transporters and reported to be important for intestinal epithelial transport, i.e., system $B^0$ ($B^0AT1$) [9,10], system ASC (ASCT2) [21], system $b^{0,+}$ ($b^{0,+}AT$) [22], system L (LAT1 [23,24] and LAT2 [25–27]), system $y^+L$, ($y^+LAT1$) [28] and system A (ATA2) [29]. It

has been demonstrated that $B^0AT1$, ASCT2 and $b^{0,+}AT$ localized at the brush-border membranes of epithelial cells, whereas LAT1, LAT2, $y^+LAT1$ and ATA2 localized at the basolateral membranes.

Fig. 5 shows the mRNA expression levels along the digestive tract for the amino acid transporters localized to brush-border membranes: $B^0AT1$, ASCT2 and $b^{0,+}AT$. These three transporters exhibited distinguishable expression patterns. $B^0AT1$ mRNA levels were increased from duodenum to ileum like MDR1 mRNA levels. ASCT2 showed little expression in the small intestine, but significant expression in the large intestine (colon and rectum). In contrast, $b^{0,+}AT$ exhibited little expression in the digestive tract except for the stomach.

Fig. 6 shows the mRNA expression levels along the digestive tract for the amino acid transporters localized to basolateral membranes: LAT1, LAT2, $y^+LAT1$ and ATA2. ATA2 showed a strong expression in the tissues tested. LAT1 was preferentially expressed in the esophagus, stomach and pancreas, as compared with the small and large intestine. The expression of LAT2 was abundant in the stomach and rectum, and modest in the small intestine
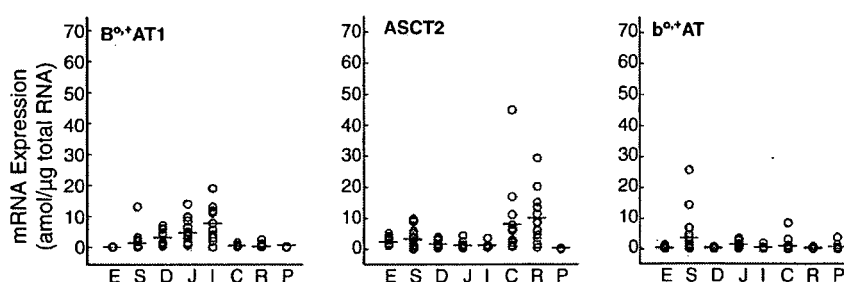


Fig. 5. mRNA expression of brush-border membrane-localized amino acid transporters $B^0AT1$, ASCT2 and $b^{0,+}AT$ along the digestive tract and pancreas. Abbreviations for each tissue and experimental methods are identical to those in Fig. 1.
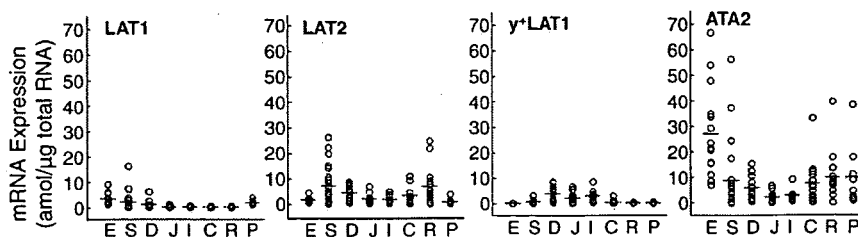


Fig. 6. mRNA expression of basolateral membrane-localized amino acid transporters LAT1, LAT2, $y^+LAT1$ and ATA2 along the digestive tract and pancreas. Abbreviations for each tissue and experimental methods are identical to those in Fig. 1.
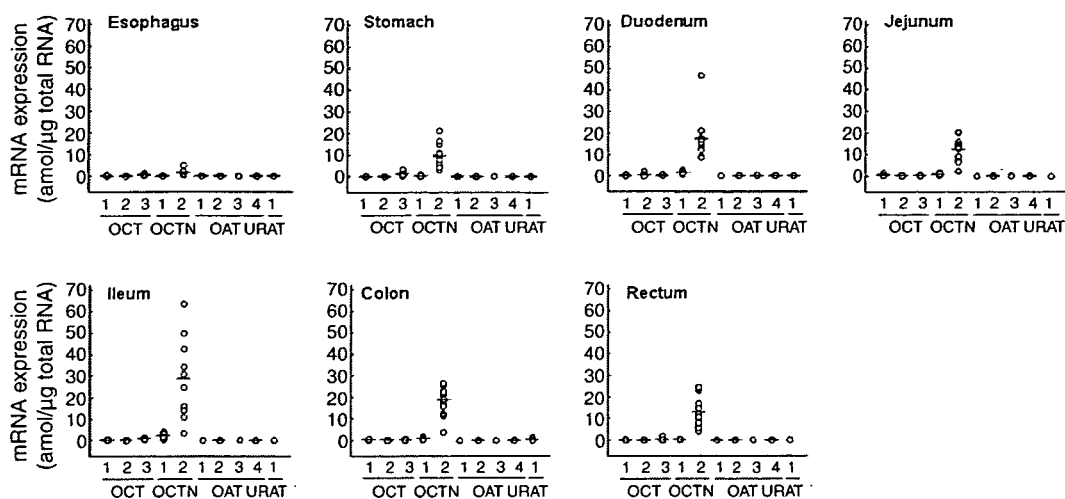
Fig. 7. mRNA expression of organic ion transporters along the digestive tract. Tested transporters are as follows: OCT1–3, OCTN1 and 2, OAT1–4 and URAT1. Experimental methods are identical to those in Fig. 1.

(duodenum, jejunum and ileum). In contrast, y$^+$LAT1 was predominantly expressed in the small intestine (duodenum, jejunum and ileum) with little expression in other tissues.

PEPT1 also works as a drug transporter. To compare the mRNA expression level of PEPT1 with other drug transporters, we selected organic ion transporter family including organic cation transporters (OCT1–3), organic cation/carnitine transporters (OCTN1 and 2), organic anion transporters (OAT1–4) and urate transporter (URAT1). These transporters are mainly expressed in the kidney [11] and play important roles for renal secretion of ionic drugs [30], but some transporters were suggested to mediate the intestinal secretion of drugs [31]. As shown in Fig. 7, there was little expression for organic ion transporters except for OCTN2. OCTN2 exhibited a similar expression level of PEPT1 in the intestine. In addition to intestine, OCTN2 exhibited abundant expression in the stomach, colon and rectum.

## 4. Discussion

In the present study, we have demonstrated that the mRNA expression level of PEPT1 is higher in the duodenum and jejunum than that of B$^0$AT1, ASCT2 and b$^{0,+}$AT, which are localized at the brush-border membranes, and is equal to that of B$^0$AT1 in the ileum. Previous works showed that luminal contents after protein ingestion mostly consist of two to six amino acids [32], and that most of the dipeptidase activity is located in the cytoplasm of mucosal cells [33]. Thus, higher expression levels of PEPT1 than amino acid transporters at brush-border membranes should support the nutritional importance of the intestinal absorption of small peptides for protein nutrition. The high expression levels of intestinal PEPT1 also emphasize the pharmacological implication of peptide transporters. The peptide-like drugs transported by PEPT1 showed good oral

bioavailability [3]. Transport abilities of PEPT1, with great flexibility for structural modification, and high expression of PEPT1 in the small intestine should be helpful for drug development to improve the intestinal absorption of poorly absorbed drugs.

The expression level of PEPT1 mRNA showed a peak in the duodenum, and gradually decreased to the ileum. Interestingly, the expression gradient of B$^0$AT1 mRNA is completely inversed to that of PEPT1. These reciprocal axial gradients in the mRNA expression of PEPT1 and B$^0$AT1 well correspond to the transport activities of small peptides [34,35] and amino acids for system B [36], and may have physiological relevance and importance to the maintenance of optimal protein nutrition [37]. Namely, the ingested proteins are digested by the membrane-bound peptidases to generate a major portion of the absorbable products, namely, amino acids and small peptides. Though these peptidases are present throughout the small intestine, levels of activity are much higher in the ileum than in the jejunum [38], indicating that the concentrations of free amino acids in the lumen are gradually increased, while the luminal concentration of small peptides are gradually decreased as the luminal contents move along the intestine. Furthermore, $K_m$ values of typical substrates for PEPT1 (glycylsarcosine) [39] and B$^0$AT1 (leucine) [10] were about 1 mM, suggesting that both transporters have similar kinetic parameters. It is, therefore, suggested that the efficient absorption of digestive products of proteins may be achieved by a good correlation between the expression profiles for PEPT1 and B$^0$AT1 and the luminal concentrations of the corresponding substrates along the intestine.

Using tissue biopsy samples, Gutmann et al. [40] demonstrated that the mRNA expression of human breast cancer resistance protein (BCRP) was maximal in the duodenum and decreased continuously down to the rectum [40]. This expression profile is contrast to that of MDR1 mRNA expression (Fig. 1 right), suggesting that BCRP and

MDR1 also complement the transport function each other along the digestive tract as the substrate specificity of both transporters is partially overlapping [41]. Taken together, reciprocal expression of functionally related membrane transporters along the digestive tract should be responsible for the efficient biological systems in physiology and pharmacology.

Recently, Dave et al. [42] examined the expression of heteromeric amino acid transporters along the murine intestine. Their major findings related to our study were as follows: (i) the main sites of mRNA expression of absorptive amino acid transporters ($b^{0,+}$AT, LAT2 and $y^{+}$LAT1) were the jejunum and ileum; (ii) a substantial level of LAT2 mRNA was found in the stomach, an organ not previously recognized as a major site of amino acid absorption and (iii) LAT1 was most abundant in brain and weakly expressed in the intestine except for the stomach. Most of these findings were also confirmed in the human intestine, although the expression levels of $b^{0,+}$AT, LAT2 and $y^{+}$LAT1were not so high in the human intestine as compared to mouse intestine. Mutations in $b^{0,+}$AT lead to the hereditary disease cystinuria [22], and characterized by renal loss and altered intestinal absorption of cationic amino acids and cystine. Interestingly, patients with cystinuria do not exhibit obvious symptoms of protein malabsorption because the affected amino acids are absorbed adequately in the form of small peptides [43]. The much higher levels of PEPT1 than $b^{0,+}$AT explain this compensation.

In the present study, PEPT1 was found to be expressed in the stomach, induced by intestinal metaplasia. Intestinal metaplasia is characterized by the transdifferentiation of gastric epithelial cells to an intestinal phenotype [19]. Several intestinal-specific gene products such as trefoil peptides [44] were reported to be expressed in the stomach after intestinal metaplasia. *CDX2*, an intestine-specific transcription factor belonging to the *caudal*-related homeobox gene family, was involved in the induction of intestinal metaplasia of the stomach [45]. We have recently clarified the significant role of Sp1 in the basal transcriptional regulation of PEPT1 [46], but the mechanisms of intestine-specific expression of PEPT1 have not been clarified yet. CDX2 may also be responsible for the small intestinal and gastric expression of PEPT1.

Among organic ion transporters tested, only OCTN2 showed significant expression in the intestine, as the same expression level of PEPT1. The physiological substrate for OCTN2 is the carnitine, and mutations in this protein cause the autosomal recessive systemic carnitine deficiency [47]. In addition to carnitine, OCTN2 can transport various drugs such as verapamil [48]. This transport activity and abundant expression in the intestine suggested the pharamcokinetic role of OCTN2 for intestinal absorption like PEPT1. Using *Oct1* knockout mice, it was demonstrated that Oct1 plays important roles for intestinal excretion of cationic drugs [49]. But, the present expression analyses

revealed that there was little expression of OCT1 along the digestive tract. Further studies are needed to clarify the clinical implication of intestinal OCT1.

In conclusion, we demonstrated the expression profile of PEPT1, amino acid transporters and organic ion transporters along the human digestive tract. The reciprocal distribution of PEPT1 and $B^{0}$AT1 may contribute to the efficient absorption of digestive products of ingested proteins. PEPT1 expression in the stomach is caused by intestinal metaplasia. OCTN2 is also abundantly expressed in the intestine. These findings may provide useful information about enteral nutrition, gastric pathology and pharmacology.

## Acknowledgements

## References

[1] Adibi SA. The oligopeptide transporter (Pept-1) in human intestine: biology and function. Gastroenterology 1997;113:332–40.

[2] Daniel H. Molecular and integrative physiology of intestinal peptide transport. Annu Rev Physiol 2004;66:361–84.

[3] Terada T, Inui K. Peptide transporters: structure, function, regulation and application for drug delivery. Curr Drug Metab 2004;5:85–94.

[4] Christensen HN. Role of amino acid transport and countertransport in nutrition and metabolism. Physiol Rev 1990;70:43–77.

[5] Verrey F, Closs EI, Wagner CA, Palacin M, Endou H, Kanai Y. CATs and HATs: the SLC7 family of amino acid transporters. Pflugers Arch 2004;447:532–42.

[6] Verrey F, Ristic Z, Romeo E, Ramadam T, Makrides V, Dave MH, et al. Novel renal amino acid transporters. Annu Rev Physiol 2005;67:557–72.

[7] Stevens BR, Ross HJ, Wright EM. Multiple transport pathways for neutral amino acids in rabbit jejunal brush border vesicles. J Membr Biol 1982;66:213–25.

[8] Munck BG, Munck LK. Phenylalanine transport in rabbit small intestine. J Physiol 1994;480:99–107.

[9] Seow HF, Broer S, Broer A, Bailey CG, Potter SJ, Cavanaugh JA, et al. Hartnup disorder is caused by mutations in the gene encoding the neutral amino acid transporter SLC6A19. Nat Genet 2004;36:999–1002.

[10] Kleta R, Romeo E, Ristic Z, Ohura T, Stuart C, Arcos-Burgos M, et al. Mutations in SLC6A19, encoding $B^{0}$AT1, cause Hartnup disorder. Nat Genet 2004;36:1003–7.

[11] Motohashi H, Sakurai Y, Saito H, Masuda S, Urakami Y, Goto M, et al. Gene expression levels and immunolocalization of organic ion transporters in the human kidney. J Am Soc Nephrol 2002;13:866–74.

[12] Masuda S, Uemoto S, Goto M, Fujimoto Y, Tanaka K, Inui K. Tacrolimus therapy according to mucosal MDR1 levels in small-bowel transplant recipients. Clin Pharmacol Ther 2004;75:352–61.

[13] Ashida K, Katsura T, Motohashi H, Saito H, Inui K. Thyroid hormone regulates the activity and expression of the peptide transporter PEPT1 in Caco-2 cells. Am J Physiol Gastrointest Liver Physiol 2002;282: G617–23.

[14] Hashida T, Masuda S, Uemoto S, Saito H, Tanaka K, Inui K. Pharmacokinetic and prognostic significance of intestinal MDR1 expression in recipients of living-donor liver transplantation. Clin Pharmacol Ther 2001;69:308–16.

[15] Zimmermann C, Gutmann H, Hruz P, Gutzwiller JP, Beglinger C, Drewe J. Mapping of MDR1 and MRP1–5 mRNA expression along the human intestinal tract. Drug Metab Dispos 2005;33:219–24.

[16] Mouly S, Paine MF. P-glycoprotein increases from proximal to distal regions of human small intestine. Pharm Res 2003;20:1595–9.

[17] Fojo AT, Ueda K, Slamon DJ, Poplack DG, Gottesman MM, Pastan I. Expression of a multidrug-resistance gene in human tumors and tissues. Proc Natl Acad Sci USA 1987;84:265–9.

[18] Ogihara H, Saito H, Shin BC, Terada T, Takenoshita S, Nagamachi Y, et al. Immuno-localization of H⁺/peptide cotransporter in rat digestive tract. Biochem Biophys Res Commun 1996;220:848–52.

[19] Fenoglio-Preiser CM, Lantz PE, Listrom MB, Davis M, Rilke FO. Metaplasia. Gastrointestinal pathology: an atlas and text. New York: Raven, 1989. p. 154–7.

[20] Trejdosiewicz LK, Malizia G, Oakes J, Losowsky MS, Janossy G. Expression of the common acute lymphoblastic leukaemia antigen (CALLA gp100) in the brush border of normal jejunum and jejunum of patients with coeliac disease. J Clin Pathol 1985;38:1002–6.

[21] Kekuda R, Prasad PD, Fei YJ, Torres-Zamorano V, Sinha S, Yang-Feng TL, et al. Cloning of the sodium-dependent, broad-scope, neutral amino acid transporter B⁰ from a human placental choriocarcinoma cell line. J Biol Chem 1996;271:18657–61.

[22] Feliubadalo L, Font M, Purroy J, Rousaud F, Estivill X, Nunes V, et al. Non-type I cystinuria caused by mutations in SLC7A9, encoding a subunit (b⁰,⁺AT) of rBAT, International Cystinuria Consortium. Nat Genet 1999;23:52–7.

[23] Kanai Y, Segawa H, Miyamoto K, Uchino H, Takeda E, Endou H. Expression cloning and characterization of a transporter for large neutral amino acids activated by the heavy chain of 4F2 antigen (CD98). J Biol Chem 1998;273:23629–32.

[24] Mastroberardino L, Spindler B, Pfeiffer R, Skelly PJ, Loffing J, Shoemaker CB, et al. Amino-acid transport by heterodimers of 4F2hc/CD98 and members of a permease family. Nature 1998;395:288–91.

[25] Pineda M, Fernandez E, Torrents D, Estevez R, Lopez C, Camps M, et al. Identification of a membrane protein, LAT-2, that co-expresses with 4F2 heavy chain, an L-type amino acid transport activity with broad specificity for small and large zwitterionic amino acids. J Biol Chem 1999;274:19738–44.

[26] Segawa H, Fukasawa Y, Miyamoto K, Takeda E, Endou H, Kanai Y. Identification and functional characterization of a Na⁺-independent neutral amino acid transporter with broad substrate selectivity. J Biol Chem 1999;274:19745–51.

[27] Rossier G, Meier C, Bauch C, Summa V, Sordat B, Verrey F, et al. LAT2, a new basolateral 4F2hc/CD98-associated amino acid transporter of kidney and intestine. J Biol Chem 1999;274:34948–54.

[28] Torrents D, Mykkanen J, Pineda M, Feliubadalo L, Estevez R, de Cid R, et al. Identification of SLC7A7, encoding y⁺LAT-1, as the lysinuric protein intolerance gene. Nat Genet 1999;21:293–6.

[29] Sugawara M, Nakanishi T, Fei YJ, Huang W, Ganapathy ME, Leibach FH, et al. Cloning of an amino acid transporter with functional characteristics and tissue expression pattern identical to that of system A. J Biol Chem 2000;275:16473–7.

[30] Inui K, Masuda S, Saito H. Cellular and molecular aspects of drug transport in the kidney. Kidney Int 2000;58:944–58.

[31] Jonker JW, Schinkel AH. Pharmacological and physiological functions of the polyspecific organic cation transporters: OCT1, 2 and 3 (SLC22A1–3). J Pharmacol Exp Ther 2004;308:2–9.

[32] Adibi SA, Mercer DW. Protein digestion in human intestine as reflected in luminal, mucosal, and plasma amino acid concentrations after meals. J Clin Invest 1973;52:1586–94.

[33] Kim YS, Birtwhistle W, Kim YW. Peptide hydrolases in the brush border and soluble fractions of small intestinal mucosa of rat and man. J Clin Invest 1972;51:1419–30.

[34] Crampton RF, Lis MT, Matthews DM. Sites of maximal absorption and hydrolysis of two dipeptides by rat small intestine in vivo. Clin Sci 1973;44:583–94.

[35] Schedl HP, Burston D, Taylor E, Matthews DM. Kinetics of mucosal influx of glycylsarcosine, glycine and leucine into hamster jejunum and ileum in vitro. Clin Sci (Lond) 1979;56:25–31.

[36] Munck LK, Munck BG. Variation in amino acid transport along the rabbit small intestine. Mutual jejunal carriers of leucine and lysine. Biochim Biophys Acta 1992;1116:83–90.

[37] Ganapathy V, Brandsch M, Leibach FH. Intestinal transport of amino acids and proteins. In: Johnson LR, editor. Physiology of the gastrointestinal tract. 3rd ed., New York: Raven; 1994. p. 1773–94.

[38] Das M, Radhakrishnan AN. A comparative study of the distribution of soluble and particulate glycyl-L-leucine hydrolase in the small intestine. Clin Sci Mol Med 1974;46:501–10.

[39] Terada T, Sawada K, Saito H, Hashimoto Y, Inui K. Functional characteristics of basolateral peptide transporter in the human intestinal cell line Caco-2. Am J Physiol 1999;276:G1435–41.

[40] Gutmann H, Hruz P, Zimmermann C, Beglinger C, Drewe J. Distribution of breast cancer resistance protein (BCRP/ABCG2) mRNA expression along the human GI tract. Biochem Pharmacol 2005;70:695–9.

[41] Litman T, Brangi M, Hudson E, Fetsch P, Abati A, Ross DD, et al. The multidrug-resistant phenotype associated with overexpression of the new ABC half-transporter, MXR (ABCG2). J Cell Sci 2000;113:2011–21.

[42] Dave MH, Schulz N, Zecevic M, Wagner CA, Verrey F. Expression of heteromeric amino acid transporters along the murine intestine. J Physiol 2004;558:597–610.

[43] Hellier MD, Holdsworth CD, Perrett D, Thirumalai C. Intestinal depeptide transport in normal and cystinuric subjects. Clin Sci 1972;43:659–68.

[44] Leung WK, Yu J, Chan FK, To KF, Chan MW, Ebert MP, et al. Expression of trefoil peptides (TFF1, TFF2, and TFF3) in gastric carcinomas, intestinal metaplasia, and non-neoplastic gastric tissues. J Pathol 2002;197:582–8.

[45] Yuasa Y. Control of gut differentiation and intestinal-type gastric carcinogenesis. Nat Rev Cancer 2003;3:592–600.

[46] Shimakura J, Terada T, Katsura T, Inui K. Characterization of the human peptide transporter PEPT1 promoter: Sp1 functions as a basal transcriptional regulator of human PEPT1. Am J Physiol Gastrointest Liver Physiol 2005;289:G471–7.

[47] Nezu J, Tamai I, Oku A, Ohashi R, Yabuuchi H, Hashimoto N, et al. Primary systemic carnitine deficiency is caused by mutations in a gene encoding sodium ion-dependent carnitine transporter. Nat Genet 1999;21:91–4.

[48] Ohashi R, Tamai I, Yabuuchi H, Nezu J, Oku A, Sai Y, et al. Na⁺-dependent carnitine transport by organic cation transporter (OCTN2): its pharmacological and toxicological relevance. J Pharmacol Exp Ther 1999;291:778–84.

[49] Jonker JW, Wagenaar E, Mol CA, Buitelaar M, Koepsell H, Smit JW, et al. Reduced hepatic uptake and intestinal excretion of organic cations in mice with a targeted disruption of the organic cation transporter 1 (Oct1 [Slc22a1]) gene. Mol Cell Biol 2001;21:5471–7.

ELSEVIER

**Biochemical Pharmacology**

# Association between tubular toxicity of cisplatin and expression of organic cation transporter rOCT2 (Slc22a2) in the rat

Atsushi Yonezawa, Satohiro Masuda, Kumiko Nishihara,
Ikuko Yano, Toshiya Katsura, Ken-ichi Inui *

*Department of Pharmacy, Kyoto University Hospital, Faculty of Medicine,
Sakyo-ku, Kyoto 606-507, Japan*

## Abstract

Cisplatin is an effective anticancer drug, but has its severe adverse effects, especially nephrotoxicity. The molecular mechanism of cisplatin-induced nephrotoxicity is still not clear. In the present study, we examined the role of rat (r)OCT2, an organic cation transporter predominantly expressed in the kidney, in the tubular toxicity of cisplatin. Using HEK293 cells stably expressing rOCT2 (HEK-rOCT2), we evaluated the cisplatin-induced release of lactate dehydrogenase and the uptake of cisplatin. The release of lactate dehydrogenase and the accumulation of platinum were greater in HEK-rOCT2 cells treated with cisplatin than in mock-transfected cells. Moreover, cimetidine and corticosterone, OCT2 inhibitors, inhibited the cytotoxicity and the transport of cisplatin in HEK-rOCT2 cells. Pharmacokinetics of cisplatin was investigated in male and female rats because the renal expression level of rOCT2 was higher in male than female rats. The renal uptake clearance of cisplatin was greater in male than female rats, while the hepatic uptake clearance was similar between the sexes. In addition, glomerular filtration rate and liver function were unchanged, but $N$-acetyl-$\beta$-D-glucosaminidase activity in the bladder urine and the urine volume were markedly increased 2 days after the administration of 2 mg/kg of cisplatin in male rats. Moreover, cisplatin did not induce the elevation of urinary $N$-acetyl-$\beta$-D-glucosaminidase activity in the castrated male rats whose renal rOCT2 level was lower than that of the sham-operated rats. In conclusion, the present results indicated that renal rOCT2 expression was the major determinant of cisplatin-induced tubular toxicity.
© 2005 Elsevier Inc. All rights reserved.

*Keywords:* Cisplatin; Organic cation transporter 2; Nephrotoxicity; Cytotoxicity; Renal tubular epithelial cells; Pharmacokinetics

## 1. Introduction

*cis*-Diamminedichloroplatinum II (CDDP, cisplatin) is widely used to treat solid tumors of prostate, bladder, colon, lung, testis and brain. Although cisplatin is an effective anticancer agent, severe nephrotoxicity limits its clinical application. It was reported that an increase in the serum creatinine concentration was observed in 41% of patients treated with high-dose cisplatin [1]. However, the major site of cisplatin-induced renal injury is the proximal tubule [2]. In addition, cisplatin induced tubular toxicity, followed by an increase in the serum creatinine

level [3]. Moreover, the tubular toxicity caused a decrease in the glomerular filtration rate (GFR), resulting in acute renal failure [4]. Therefore, it was suggested that cisplatin was toxic primarily to renal tubular epithelial cells. But, the molecular mechanism of cisplatin-induced nephrotoxicity is still unknown.

Safirstein et al. [5] reported that cisplatin was concentrated in rat renal cortical slices five-fold above the concentration in medium. We previously demonstrated that cisplatin treatment from the basolateral side caused sever toxicity compared to the apical side in the porcine derived epithelial cell line LLC-PK₁ cells [6]. Recently, Ludwig et al. [7] reported that cisplatin-induced cytotoxicity was specifically observed from the basolateral side, and the toxicity was ameliorated in the presence of cimetidine in

* Corresponding author. Tel.: +81 75 751 3577; fax: +81 75 751 4207.
*E-mail address:* inui@kuhp.kyoto-u.ac.jp (K.-i. Inui).

Madin-Darby canine kidney (MDCK) cells. These reports suggested that the uptake of cisplatin in tubular epithelial cells was mediated by basolateral drug transporter(s). Identification of the transporter(s) is essential to understand the mechanism of cisplatin-induced nephrotoxicity.

Human organic cation transporter 2 (hOCT2) is the most abundant organic cation transporter in the kidney among an organic cation transporter family which consists of hOCT1-3 (SLC22A1-3) and hOCTN1 and 2 (SLC22A4 and 5) [8,9]. Rat (r)OCT2 is expressed predominantly in the basolateral membranes of proximal tubules and mediated the accumulation of various cationic drugs into proximal tubular epithelial cells from the circulation [10–14]. Uptake of tetraethylammonium (TEA) by rOCT2 was suppressed by the replacement of $Na^+$ with $K^+$, suggesting that the transport activity of rOCT2 was membrane potential-dependent [9, 15]. Based on such backgrounds and findings, we hypothesized that rOCT2 was the key molecule to clarifying the tubular accumulation and subsequent nephrotoxicity of cisplatin.

In the present study, we investigated whether rOCT2 affected the nephrotoxicity of cisplatin in rat proximal tubules. We examined the effect of rOCT2 expression on the cytotoxicity of cisplatin in HEK293 transfectants and on the pharmacokinetics of cisplatin in rats.

## 2. Materials and methods

### 2.1. Cell culture and transfection

HEK293 cells (American Type Culture Collection CRL-1573) were cultured in complete medium consisting of Dulbecco's modified Eagle's medium (Sigma Chemical Co., St. Louis, MO) with 10% fetal bovine serum (Whittaker Bioproducts Inc., St. Louis, MO) in an atmosphere of 5% $CO_2$–95% air at 37 °C.

The construction of HEK293 cells stably expressing rOCT2 (HEK-rOCT2) was performed as described [14]. The transfectants were used for the experiments at 48 h after seeding.

For a transient expression system, pBK-CMV plasmid vector DNA (Stratagene, La Jolla, CA), containing rOCT1 or rOCT2 cDNA, was purified using Wizard® Plus SV Minipreps DNA Purification System (Promega, San Luis Obispo, CA). The day before transfection, HEK293 cells were seeded onto poly-D-lysine-coated 24-well plates at a density of 2.0 × 10⁵ cells per well. The cells were transfected with 50 ng of total plasmid DNA per well using 0.125 μl of LipofectAMINE 2000 (Invitrogen, Carlsbad, CA) per well according to the manufacturer's instructions. Forty-eight hours after the transfection, the cells were used for uptake experiments.

### 2.2. Uptake experiment

Cellular uptake of [¹⁴C]TEA (88.8 MBq/mmol, Perkin-Elmer Inc., Wellesley, MA) was measured with monolayer cultures grown on poly-D-lysine-coated 24-well plates. The composition of the incubation buffer was as follows: 145 mM NaCl, 3 mM KCl, 1 mM $CaCl_2$, 0.5 mM $MgCl_2$, 5 mM D-glucose and 5 mM HEPES (pH 7.4 adjusted with NaOH). Experimental procedures were performed as described previously [14].

For the measurement of cisplatin uptake, seeded cells were incubated with the medium containing cisplatin with or without cimetidine or corticosterone for 1 h. After this incubation, the monolayers were rapidly washed twice with ice-cold incubation buffer containing 1% bovine serum albumin (Nacalai Tesque, Kyoto, Japan) and then washed three times with ice-cold incubation buffer. The cells were solubilized in 0.5N NaOH, and the amount of platinum was determined using inductively coupled plasma-mass spectrometry (ICP-MS) by the Pharmacokinetics and Bioanalysis Center, Shin Nippon Biomedical Laboratories, Ltd. (Wakayama, Japan).

The protein content of the cell monolayers solubilized in 0.5N NaOH was determined by the method of Bradford with a Bio-Rad Protein Assay Kit (Bio-Rad Laboratories, Richmond, CA).

### 2.3. Cytotoxicity experiment

The cytotoxicity of cisplatin was measured with monolayer cultures grown on poly-D-lysine-coated 12-well plates. Cells were incubated with the medium containing cisplatin with or without cimetidine or corticosterone for 2 h. After removal of the medium, drug-free medium was added. After incubation for 24 h, the medium was collected, and the lactate dehydrogenase (LDH) activity in the medium was measured using a LDH Cytotoxicity Detection Kit (Takara, Shiga, Japan), according to the manufacturer's instructions. Cytotoxicity was evaluated by measuring LDH activity in the medium. Total LDH activity was defined as LDH activity in the medium containing 1% TritonX-100. LDH release represents (LDH activity − LDH activity of control)/(total LDH activity − LDH activity of control).

### 2.4. Quantification of mRNA expression

Cellular total RNA was extracted using a MagNA Pure LC RNA isolation kit II (Roche Diagnostic GmbH, Mannheim, Germany) [8]. The total RNA was reverse-transcribed, and the single stranded DNA was used for the quantification of mRNA expression.

Real-time PCR was performed in a total volume of 20 μl containing 2 μl of reverse-transcribed cDNA, 1 μM forward and reverse primers, 0.2 μM TaqMan probe, and 10 μl of TaqMan Universal PCR Master Mix (Applied

Biosystems, Foster City, CA). The quantification of mRNA was performed as reported [8].

### 2.5. Pharmacokinetics of cisplatin

The pharmacokinetics experiment was performed using male or female Wistar/ST rats (8 weeks), as described previously with some modifications [16]. Cisplatin (0.5 mg/kg) was administered as a bolus via the catheterized right femoral vein. Blood samples were collected at 0.5, 1, 1.5, 2, 2.5 and 3 min from the left femoral artery. Three minutes after the injection, the kidney and liver were collected immediately after sacrificing the rats. The excised tissues were gently washed, weighed and homogenized in 3 volumes of 0.9% NaCl. The amounts of cisplatin were measured by ICP-MS. The animal experiments were performed in accordance with the "Guidelines for Animal Experiments of Kyoto University". All protocols were previously approved by the Animal Research Committee, Graduate School of Medicine, Kyoto University.

### 2.6. Western blot analysis

The crude membrane fractions were prepared from rat kidneys as described previously [17]. The crude membrane fractions (25 μg) were separated by 10% sodium dodecyl sulphate-polyacrylamide gel electrophoresis (SDS-PAGE) and transferred onto polyvinylidene difluoride membranes (Immobilon-P®, Millipore, Bedford, MA) by semi-dry electroblotting. The blots were blocked and incubated overnight at 4 °C with each primary antibody specific for rOCT2 [18], or the $Na^+/K^+$-ATPase α1 subunit (Upstate Biotechnology Inc., Lake Placid, NY). The bound antibody was detected on X-ray film using enhanced chemiluminescence (ECL) with horseradish peroxidase-conjugated secondary antibodies and cyclic diacylhydrazides (Amersham Pharmacia Biotech, Uppsala, Sweden).

### 2.7. Acute renal failure

Male Wistar/ST rats (8 weeks) were used or male rats (5 weeks) were surgically castrated 3 weeks before the experiment. Acute renal failure was induced by intraperitoneal administration of 2 mg/kg of cisplatin. Rats were maintained in metabolic cages for 24 h before the experiment to determine urine output and the urinary level of creatinine. Two days after the administration of cisplatin, plasma and bladder urine samples were collected and then the state of the kidneys was determined, as previously described [19]. The liver function data were determined using the assay kits from Wako Pure Chemical Industries (Osaka, Japan). The concentration of testosterone was measured using an ELISA kit (Cayman Chemical Co., Ann Arbor, MI).

### 2.8. Statistical analysis

Data are expressed as means ± S.E.M. Data were analyzed statistically using the unpaired Student $t$ test. Multiple comparisons were performed with Dunnett's two-tailed test after a one-way ANOVA. Probability values of less than 0.05 were considered statistically significant.

## 3. Results

### 3.1. Uptake of TEA by HEK293 cells stably expressing rOCT2

We constructed HEK293 cells stably transfected with the pBK-CMV vector or rOCT2-containing vector (HEK-pBK or HEK-rOCT2). To check the function of these cells, the cellular uptake of [$^{14}$C]TEA by HEK-pBK cells or HEK-rOCT2 cells was measured. The amounts of [$^{14}$C]TEA in HEK-pBK cells and HEK-rOCT2 cells were 19.2 ± 4.0 and 317.4 ± 11.7 pmol/mg protein/2 min, respectively. Therefore, these cells were used in the subsequent experiments.

### 3.2. Cytotoxicity of cisplatin in HEK-pBK cells and HEK-rOCT2 cells

We compared the sensitivities of HEK-pBK cells and HEK-rOCT2 cells to cisplatin (Fig. 1). When HEK-pBK cells were treated with 30–300 μM cisplatin for 2 h and subsequently cultured in normal medium for 24 h, the release of LDH into the culture medium was not significantly enhanced. Treatment with 1000 μM cisplatin promoted the release of LDH in HEK-pBK cells. On the other hand, when HEK-rOCT2 cells were treated with 30–1000 μM cisplatin, the amount of LDH released increased in a dose-dependent manner. The release of LDH was greater in HEK-rOCT2 cells treated with 30–1000 μM cisplatin than in HEK-pBK cells (Fig. 1A). Further, we investigated the effects of OCT2 inhibitors, cimetidine and corticosterone, on the cisplatin-induced cytotoxicity. The cytotoxicity of cisplatin was completely inhibited in the presence of 1 mM cimetidine or 100 μM corticosterone in HEK-rOCT2 cells (Fig. 1B).

### 3.3. Transport of cisplatin by HEK-pBK cells and HEK-rOCT2 cells

To investigate whether rOCT2 recognizes cisplatin as its substrate, the effect of cisplatin on the uptake of [$^{14}$C]TEA and the accumulation of cisplatin by HEK-rOCT2 cells were examined (Fig. 2). Cisplatin, cimetidine and corticosterone had inhibitory effects on the uptake of [$^{14}$C]TEA by HEK-rOCT2 cells in a dose-dependent manner. The $IC_{50}$ values of cisplatin, cimetidine and corticosterone were 2096.2 ± 59.5, 216.1 ± 4.5 and 2.50 ± 0.02 μM,
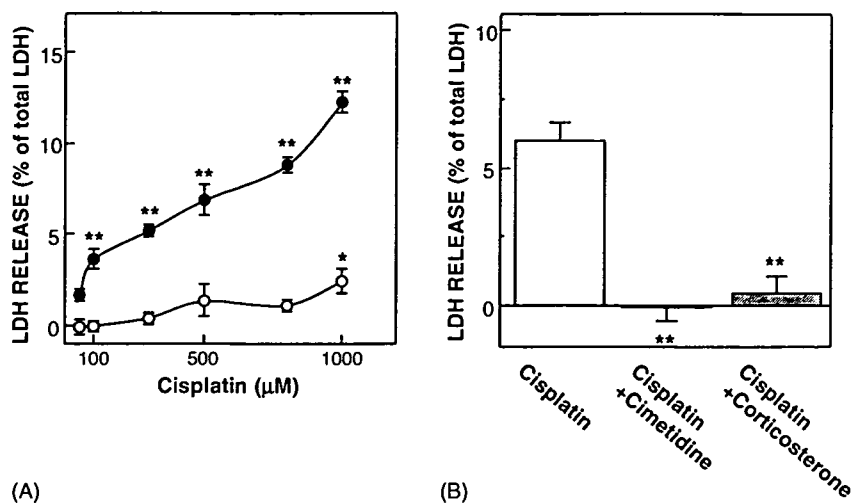
(A)    (B)

Fig. 1. Role of rOCT2 in the cytotoxicity of cisplatin. (A) Concentration-dependence of cytotoxicity in HEK-pBK cells (open circle) or HEK-rOCT2 cells (closed circle). Cells were exposed to cisplatin for 2 h, and then incubated in normal medium for 24 h. (B) Cimetidine (1 mM) or corticosterone (100 μM) was coadministrated with cisplatin (500 μM) for 2 h, and then the cells were incubated in normal medium for 24 h. Each point represents the mean ± S.E.M. of three wells. *$P < 0.05$; **$P < 0.01$, significantly different from control cells.
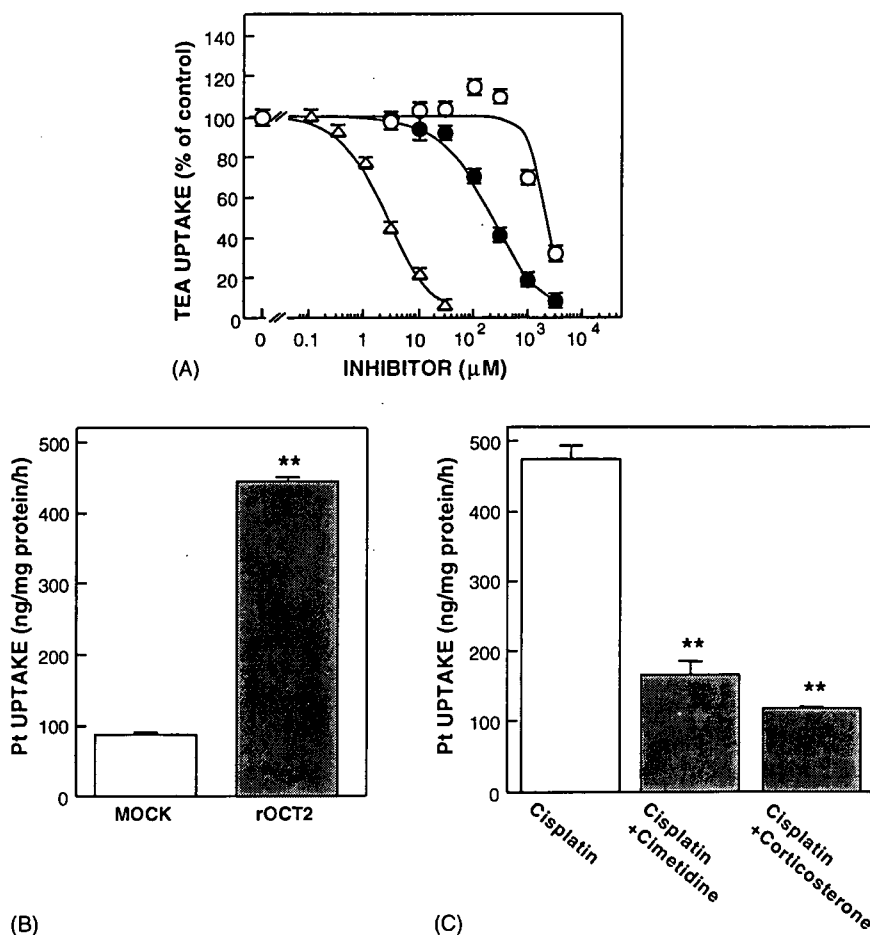


(A)    (B)    (C)

Fig. 2. Uptake of cisplatin by HEK-pBK cells or HEK-rOCT2 cells. (A) HEK-rOCT2 cells were incubated with 50 μM [$^{14}$C]TEA in the presence of cisplatin (open circle), cimetidine (closed circle) or corticosterone (open triangle) at various concentrations for 2 min. The amount of [$^{14}$C]TEA in HEK-rOCT2 cells was determined by measuring the radioactivity of solubilized cells. (B) HEK-pBK cells (MOCK) or HEK-rOCT2 cells (rOCT2) were incubated with 500 μM cisplatin for 1 h. (C) HEK-rOCT2 cells were incubated with 500 μM cisplatin in the presence or absence of 1 mM cimetidine or 100 μM corticosterone for 1 h. The amount of platinum in HEK-pBK cells or HEK-rOCT2 cells was determined by ICP-MS. Each point represents the mean ± S.E.M. of three or four wells. **$P < 0.01$, significantly different from MOCK cells or control cells.
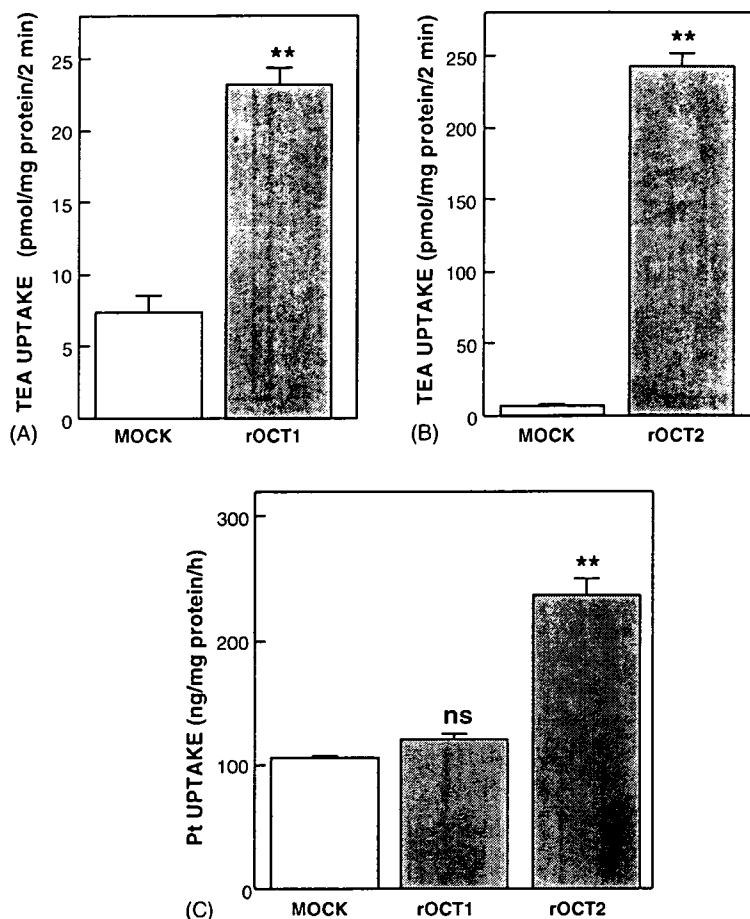
Fig. 3. rOCT1 or rOCT2-mediated uptake of cisplatin. HEK293 cells transiently expressing pBK-CMV (MOCK), rOCT1 or rOCT2 were incubated with 50 μM [$^{14}$C]TEA for 2 min (A and B) or 500 μM cisplatin for 1 h (C). The amount of [$^{14}$C]TEA or platinum was determined. Each point represents the mean ± S.E.M. of three or four wells. ns, not significantly; $^{**}P < 0.01$, significantly different from MOCK cells.

respectively (Fig. 2A). After the incubation with 500 μM cisplatin for 1 h, the amounts of platinum in HEK-pBK cells and HEK-rOCT2 cells were 90.0 ± 2.8 and 447.7 ± 5.3 ng/mg protein/h, respectively (Fig. 2B). Moreover, the accumulation of platinum by HEK-rOCT2 cells was inhibited in the presence of 1 mM cimetidine or 100 μM corticosterone (Fig. 2C).

### 3.4. Transport of cisplatin by HEK293 cells transiently expressing rOCT1 and rOCT2

Following the transfection of rOCT1 or rOCT2 cDNA, the mRNA expression levels of these transporters were 8037 ± 701 and 5834 ± 306 amol/mg protein (mean ± S.E.M. of four monolayers), respectively. Uptake of [$^{14}$C]TEA was observed in HEK293 cells transiently expressing rOCT1 or rOCT2 (Fig. 3A and B). However, the amount of platinum accumulated in the HEK293 cells transiently transfected with pBK-CMV, rOCT1 and rOCT2 was 107.8 ± 1.1, 122.4 ± 4.0 (ns versus pBK-CMV) and 237.6 ± 13.8 ($P < 0.01$ versus pBK-CMV) ng/mg protein/ h, respectively (Fig. 3C).

### 3.5. Pharmacokinetics of cisplatin in male and female rats

We compared the pharmacokinetics of cisplatin between male and female rats, because it was found that the expression level of renal rOCT2, but not rOCT1, was much higher in male rats than female rats [18]. The plasma concentrations of platinum up to 3 min after the administration of cisplatin as a bolus were determined (Fig. 4A). The total clearance (CL$_{total}$) of cisplatin, which was calculated from the dose and area under the concentration-time curve (AUC) of cisplatin for 3 min, was 35.1 ± 3.5 ml/min and 16.8 ± 1.1 ml/min in male and female rats, respectively (Fig. 4B). The tissue uptake clearance (CL$_{tissue}$), which was calculated from the AUC of cisplatin for 3 min and the amount of cisplatin in tissue at 3 min, was also examined. The renal CL$_{tissue}$ was significantly greater in male rats (13.2 ± 1.3 ml/min) than female rats (5.9 ± 0.4 ml/min). However, hepatic CL$_{tissue}$ in male rats (3.7 ± 0.3 ml/min) was not significantly different from that in female rats (2.6 ± 0.2 ml/min) (Fig. 4C). In addition, the male-dominant expression of
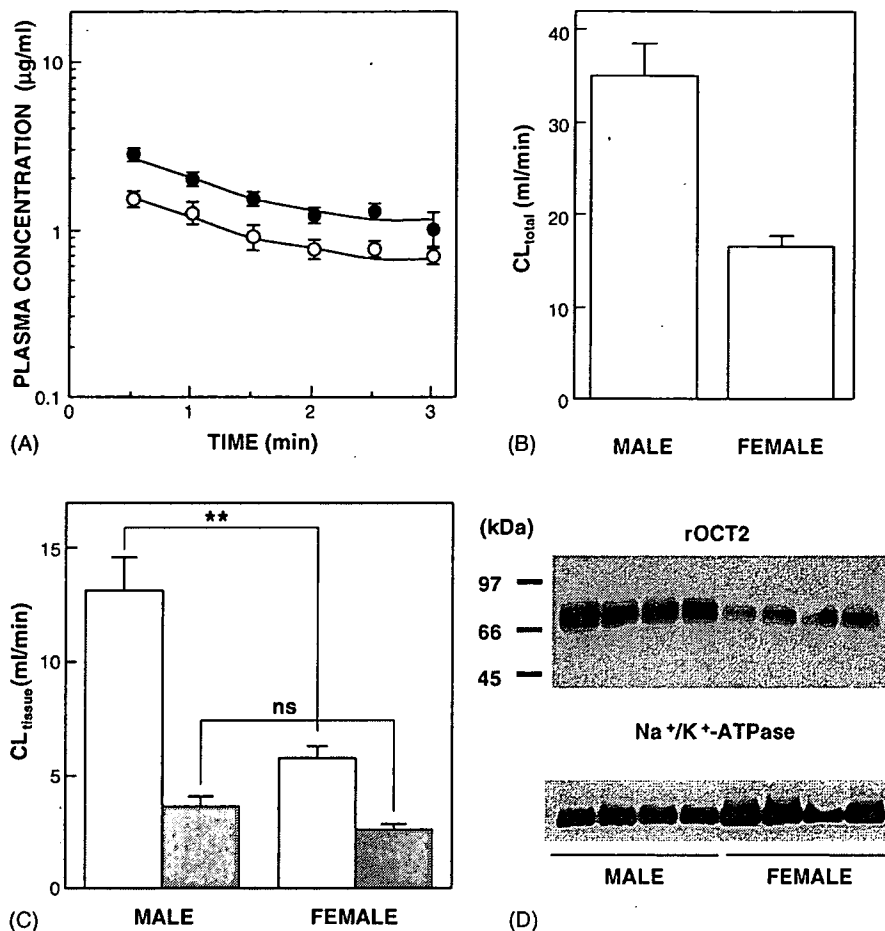
Fig. 4. Pharmacokinetics of cisplatin in male and female rats. (A) Plasma concentrations of platinum at various points were determined in male (open circle) and female (closed circle) rats. Total clearance ($CL_{total}$; B) and tissue uptake clearance ($CL_{tissue}$; C: renal $CL_{tissue}$ (open column) and hepatic $CL_{tissue}$ (closed column)) were calculated by dividing the administered dose or the amount in tissue at 3 min by the area under the curve (AUC) from 0 to 3 min, respectively. Each column represents the mean ± S.E.M. of five rats. ns, not significantly different; $^{**}P < 0.01$, significantly different. (D) Protein expression of rOCT2 and $Na^+/K^+$-ATPase in male and female rats. Representative photographs of Western blotting are shown.

the renal rOCT2 was confirmed by Western blotting (Fig. 4D).

## 3.6. Renal functional data of male rats treated with cisplatin

The male rats showed renal tubular toxicity 2 days after the administration of 2 mg/kg of cisplatin. The body weight, plasma creatinine level, creatinine clearance, blood urea nitrogen (BUN), urinary albumin level, aspartate aminotransferase (AST), alanine aminotransferase (ALT) and total bilirubin level were unaffected. However, N-acetyl-β-D-glucosaminidase (NAG) activity and urine volume were significantly increased in the male rats treated with cisplatin compared to the control rats (Table 1).

To confirm the contribution of renal rOCT2 expression on cisplatin-induced tubulotoxicity, we compared the NAG

Table 1
Biochemical parameters in male rats treated with cisplatin (2 mg/kg)

|  | Sham | Cisplatin |
| --- | --- | --- |
| Body weight (g) | 281 ± 4 | 274 ± 3 |
| Urine volume (ml/24 h) | 10.9 ± 0.9 | 22.4 ± 2.9$^{**}$ |
| NAG (U/day) | 129 ± 42 | 317 ± 47$^{**}$ |
| Pcre (mg/dl) | 0.42 ± 0.02 | 0.50 ± 0.03 |
| Ccr (ml/min/kg) | 5.81 ± 0.08 | 5.96 ± 0.06 |
| BUN (mg/dl) | 14.9 ± 0.3 | 14.2 ± 0.6 |
| Urinary albumin (mg/day) | 0.24 ± 0.06 | 0.44 ± 0.08 |
| AST (IU/l) | 61.8 ± 4.0 | 76.1 ± 6.2 |
| ALT (IU/l) | 15.0 ± 1.3 | 18.8 ± 1.7 |
| T-Bil (mg/dl) | 0.05 ± 0.01 | 0.11 ± 0.04 |

Values represent means ± S.E.M. of nine rats. NAG, N-acetyl-β-D-glucosaminidase; Pcre, plasma creatinine; Ccr, creatinine clearance; BUN, blood urea nitrogen; AST, aspartate aminotransferase; ALT, alanine aminotransferase; T-Bil, total bilirubin.
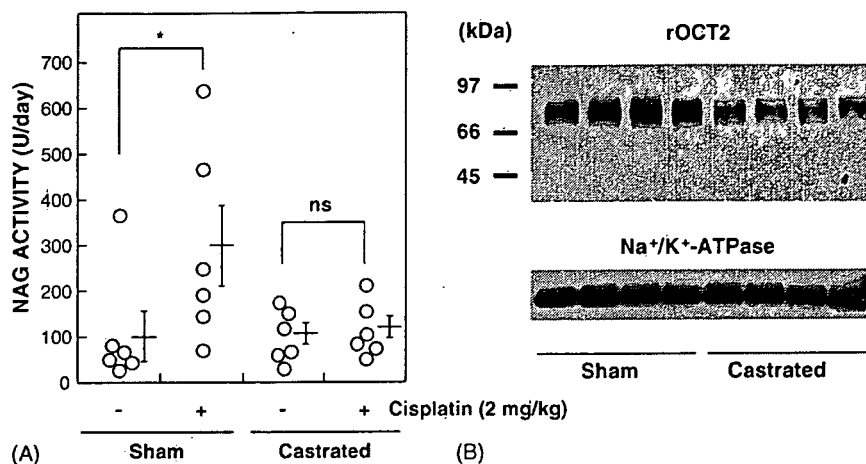$^{**}$ $P < 0.01$, significantly different from sham.

Fig. 5. Effect of the castration on cisplatin-induced tubular toxicity and renal rOCT2 expression. Male rats (5 weeks) were surgically castrated, and fed and given water freely for 3 weeks. (A) The NAG activity in bladder urine in the sham-operated or castrated rats 2 days after the administration of 2 mg/mg of cisplatin ($n = 6$). Each bar represents the mean ± S.E.M. of six rats. ns, not significantly different; $^{*}P < 0.05$, significantly different. (B) Protein expression of rOCT2 and Na$^{+}$/K$^{+}$-ATPase in the sham-operated or castrated rats. Representative photographs of Western blotting are shown.

activity in bladder urine between the sham-operated and castrated male rats. The serum concentrations of testosterone were 1.56 ± 0.11 and 0.25 ± 0.04 ng/ml (mean ± S.E.M. of 12 rats; $P < 0.01$) in the sham-operated and castrated rats, respectively. Two days after the administration of 2 mg/kg of cisplatin, NAG activity was significantly increased in the sham-operated rats. On the other hand, 2 mg/kg of cisplatin was not enough to increase urinary NAG activity in the castrated rats (Fig. 5A). The renal rOCT2 expression was decreased in the castrated rats compared to the sham-operated rats (Fig. 5B).

## 4. Discussion

Using cultured renal epithelial cells, cisplatin was found to be accumulated from the basolateral membranes via a specific carrier system [6,7,20]. In OK cells, the basolateral uptake of cisplatin was decreased in the presence of TEA [20]. Ludwig et al. [7] reported that cisplatin-induced cytotoxicity was ameliorated in the presence of cimetidine in MDCK-C7 cells. Although a polyclonal antibody against rat OCT2 (OCT2-A®, Alpha-diagnostic, San Antonio, TX) showed two signals, 65 and 50 kDa [7], the amino acid sequence of the antigen peptide was conserved 76% in mouse, 66% in porcine and 57% in human (http://www.4adi.com/data/oat/oct21.html). Therefore, the 65-kDa signal was speculated to be a canine OCT2 [7], but this should be confirmed using an actual antibody against an appropriate antigen. In the present study, we have demonstrated that rOCT2 mediated the uptake of cisplatin into the stable transfectant HEK-rOCT2 cells, and stimulated cisplatin-sensitivity in comparison with the control cells (Figs. 1 and 2). Hitherto it has not been clear which transporter protein mediated the uptake of cisplatin in renal tubular cells. The present study in vitro indicated that rOCT2 was a cisplatin transporter in the kidney.

Intracellularly, the two chlorides of cisplatin are rapidly replaced by hydroxyl groups to produce a toxic agent [21]. This agent can induce nuclear damage [22], cause mitochondrial damage [23] or trigger several other mechanisms [24], resulting in cell death. Therefore, it is considered that the entering into the cells is the most important step in the cytotoxicity of cisplatin. It was reported that the deletion of copper transporter 1 (Ctr1) resulted in resistance to cisplatin in yeast and mammal cells, and therefore, Ctr1 was suggested to be a candidate transporter mediating cisplatin uptake. [25]. On the other hand, copper-transporting P-type adenosine triphosphate (ATP7B) [26–28] and ATP-binding cassette, subfamily C2 (ABCC2, known as MRP2 or cMOAT) [29,30] promoted cisplatin efflux and had a role in cisplatin resistance. However, these three transporters were suggested to have a minor role in cisplatin-induced tubular toxicity, because the tissue distribution of these transporter proteins was not limited to the kidney, but was in the liver, intestine and brain [31–33].

Urakami et al. [18] reported that the renal expression of rOCT2, but not rOCT1, was markedly higher in male than female rats. In addition, there was a gender difference in the uptake of TEA but not p-aminohippurate, a typical substrate of organic anion transporter 1, in rat renal slices [18]. Because there is no selective and non-toxic rOCT2 antagonist, we performed the cisplatin pharmacokinetic experiments using the gender difference in the renal rOCT2 expression. It was expected that the renal distribution of cisplatin would be much greater in male than female rats. As expected, the renal CL$_{tissue}$ of cisplatin was significantly greater in male rats than female rats, while hepatic CL$_{tissue}$ did not differ between males and females. Moreover, the renal CL$_{tissue}$ was 3.5 times higher than the hepatic CL$_{tissue}$ in male rats (Fig. 4C). In addition, the transport of cisplatin was mediated by rOCT2 predominantly expressed in kidney [10], but not rOCT1 expressed

in liver, kidney and intestine [34] (Fig. 3C). These results suggested that rOCT2 played a major role in the distribution of cisplatin. As previously reported, the renal clearance of cisplatin was inhibited by cationic compounds having the potential to interact with rOCT2 such as quinidine, cimetidine and ranitidine in dogs [35]. Based on these findings, it was suggested that rOCT2 mainly mediated the tubular accumulation of cisplatin.

There are numerous reports suggesting that cisplatin causes nephrotoxicity, glomerular and tubular injury [3,19,36–38]. In these studies, cisplatin was used at dose of more than 5 mg/kg in rats, which was severe compared to clinical use. The peak concentration of cisplatin in humans undergoing chemotherapy was reported to be 3.4 μg/ml [39]. In the present study, the blood concentration of cisplatin in rats after the administration of cisplatin (0.5 mg/kg) as a bolus was between 1 and 3 μg/ml (Fig. 4A). When rats were administered 2 mg/kg of cisplatin, the activity of NAG in bladder urine and the urine volume were increased, while plasma creatinine level, creatinine clearance, BUN, urinary albumin level, AST, ALT and total bilirubin level were unchanged (Table 1). These results indicated that kidney was more sensitive to cisplatin than liver. It corresponded to the pharmacokinetics of cisplatin (Fig. 4). Kishore et al. [38] demonstrated that the polyuria after the cisplatin treatment was accompanied by decreased expression levels of aquaporin (AQP) 1 in the proximal tubules as well as AQP2 and AQP3 in the collecting ducts in rats. Using the specific antibody, rOCT2 protein was expressed in proximal tubular cells at the basolateral membrane [12] and mRNA of rOCT2 was detected abundantly in proximal tubules and weakly in distal convoluted tubules and collecting ducts [11]. Based on these findings, the proximal tubules were the most sensitive to cisplatin, because they consisted of rOCT2-rich cells.

We previously reported that testosterone increased the expression level of renal rOCT2 and stimulated TEA accumulation by kidney slices [40] and that testosterone recovered the renal rOCT2 expression and the clearance of cimetidine in chronic renal failure rats [41]. In the present study, to investigate the role of rOCT2 in cisplatin-induced tubular toxicity, we used the castrated rats as a model for the depression of rOCT2. As a result, cisplatin induced the increase of urinary NAG activity in the sham-operated rats, but not in the castrated rats whose renal rOCT2 expression was lower than the sham-operated rats (Fig. 5). In addition, cellular uptake and renal distribution of cisplatin depended on rOCT2 expression (Figs. 2B and 4). Therefore, it was suggested that rOCT2 was the determinant of the tissue distribution of cisplatin and cisplatin-induced tubular toxicity in vivo.

The tissue distribution and renal distribution of hOCT2 in humans are similar with those of rats [8,12,13]. The functional characteristics including substrate specificity of hOCT2 was consistent with rOCT2 [9]. Therefore, the present data of rOCT2 on cisplatin-induced nephrotoxicity may be reflected in humans. The renal toxicity of cisplatin

in humans should be confirmed in future focusing on hOCT2.

We propose OCT2 as the transporter responsible for cisplatin-induced renal tubular toxicity. Some OCT2-specific antagonists may prevent the nephrotoxicity of cisplatin.

## Acknowledgments

## References

[1] de Jongh FE, van Veen RN, Veltman SJ, de Wit R, van der Burg ME, van den Bent MJ, et al. Weekly high-dose cisplatin is a feasible treatment option: analysis on prognostic factors for toxicity in 400 patients. Br J Cancer 2003;88:1199–206.

[2] Dobyan DC, Levi J, Jacobs C, Kosek J, Weiner MW. Mechanism of cis-platinum nephrotoxicity. II. Morphologic observations. J Pharmacol Exp Ther 1980;213:551–6.

[3] Ichimura T, Hung CC, Yang SA, Stevens JL, Bonventre JV. Kidney injury molecule-1: a tissue and urinary biomarker for nephrotoxicant-induced renal injury. Am J Physiol Renal Physiol 2004;286:F552–3.

[4] Thadhani R, Pascual M, Bonventre JV. Acute renal failure. N Engl J Med 1996;334:1448–60.

[5] Safirstein R, Miller P, Guttenplan JB. Uptake and metabolism of cisplatin by rat kidney. Kidney Int 1984;25:753–8.

[6] Okuda M, Tsuda K, Masaki K, Hashimoto Y, Inui K. Cisplatin-induced toxicity in LLC-PK1 kidney epithelial cells: role of basolateral membrane transport. Toxicol Lett 1999;106:229–35.

[7] Ludwig T, Riethmuller C, Gekle M, Schwerdt G, Oberleithner H. Nephrotoxicity of platinum complexes is related to basolateral organic cation transport. Kidney Int 2004;66:196–202.

[8] Motohashi H, Sakurai Y, Saito H, Masuda S, Urakami Y, Goto M, et al. Gene expression levels and immunolocalization of organic ion transporters in the human kidney. J Am Soc Nephrol 2002;13:866–74.

[9] Inui K, Masuda S, Saito H. Cellular and molecular aspects of drug transport in the kidney. Kidney Int 2000;58:944–58.

[10] Okuda M, Saito H, Urakami Y, Takano M, Inui K. cDNA cloning and functional expression of a novel rat kidney organic cation transporter, OCT2. Biochem Biophys Res Commun 1996;224:500–7.

[11] Urakami Y, Okuda M, Masuda S, Akazawa M, Saito H, Inui K. Distinct characteristics of organic cation transporters, OCT1 and

OCT2, in the basolateral membrane of renal tubules. Pharm Res 2001;18:1528–34.

[12] Sugawara-Yokoo M, Urakami Y, Koyama H, Fujikura K, Masuda S, Saito H, et al. Differential localization of organic cation transporters rOCT1 and rOCT2 in the basolateral membrane of rat kidney proximal tubules. Histochem Cell Biol 2000;114:175–80.

[13] Urakami Y, Okuda M, Masuda S, Saito H, Inui K. Functional characteristics and membrane localization of rat multispecific organic cation transporters, OCT1 and OCT2, mediating tubular secretion of cationic drugs. J Pharmacol Exp Ther 1998;287:800–5.

[14] Urakami Y, Kimura N, Okuda M, Inui K. Creatinine transport by basolateral organic cation transporter hOCT2 in the human kidney. Pharm Res 2004;21:976–81.

[15] Okuda M, Urakami Y, Saito H, Inui K. Molecular mechanisms of organic cation transport in OCT2-expressing Xenopus oocytes. Biochim Biophys Acta 1999;1417:224–31.

[16] Ito T, Yano I, Masuda S, Hashimoto Y, Inui K. Distribution characteristics of levofloxacin and grepafloxacin in rat kidney. Pharm Res 1999;16:534–9.

[17] Masuda S, Saito H, Nonoguchi H, Tomita K, Inui K. mRNA distribution and membrane localization of the OAT-K1 organic anion transporter in rat renal tubules. FEBS Lett 1997;407:127–31.

[18] Urakami Y, Nakamura N, Takahashi K, Okuda M, Saito H, Hashimoto Y, et al. Gender differences in expression of organic cation transporter OCT2 in rat kidney. FEBS Lett 1999;461:339–42.

[19] Horiba N, Masuda S, Takeuchi A, Saito H, Okuda M, Inui K. Gene expression variance based on random sequencing in rat remnant kidney. Kidney Int 2004;66:29–45.

[20] Endo T, Kimura O, Sakata M. Carrier-mediated uptake of cisplatin by the OK renal epithelial cell line. Toxicology 2000;146:187–95.

[21] Goldstein RS, Mayor GH. The nephrotoxicity of cisplatin. Life Sci 1983;32:685–90.

[22] Leibbrandt ME, Wolfgang GH, Metz AL, Ozobia AA, Haskins JR. Critical subcellular targets of cisplatin and related platinum analogs in rat renal proximal tubule cells. Kidney Int 1995;48:761–70.

[23] Zhang JG, Lindup WE. Role of mitochondria in cisplatin-induced oxidative damage exhibited by rat renal cortical slices. Biochem Pharmacol 1993;45:2215–22.

[24] Wang D, Lippard SJ. Cellular processing of platinum anticancer drugs. Nat Rev Drug Discov 2005;4:307–20.

[25] Ishida S, Lee J, Thiele DJ, Herskowitz I. Uptake of the anticancer drug cisplatin mediated by the copper transporter Ctr1 in yeast and mammals. Proc Natl Acad Sci USA 2002;99:14298–302.

[26] Komatsu M, Sumizawa T, Mutoh M, Chen ZS, Terada K, Furukawa T, et al. Copper-transporting P-type adenosine triphosphatase (ATP7B) is associated with cisplatin resistance. Cancer Res 2000;60:1312–6.

[27] Miyashita H, Nitta Y, Mori S, Kanzaki A, Nakayama K, Terada K, et al. Expression of copper-transporting P-type adenosine triphosphatase (ATP7B) as a chemoresistance marker in human oral squamous cell carcinoma treated with cisplatin. Oral Oncol 2003;39:157–62.

[28] Nakayama K, Kanzaki A, Terada K, Mutoh M, Ogawa K, Sugiyama T, et al. Prognostic value of the Cu-transporting ATPase in ovarian carcinoma patients receiving cisplatin-based chemotherapy. Clin Cancer Res 2004;10:2804–11.

[29] Cui Y, Konig J, Buchholz JK, Spring H, Leier I, Keppler D. Drug resistance and ATP-dependent conjugate transport mediated by the apical multidrug resistance protein, MRP2, permanently expressed in human and canine cells. Mol Pharmacol 1999;55:929–37.

[30] Koike K, Kawabe T, Tanaka T, Toh S, Uchiumi T, Wada M, et al. A canalicular multispecific organic anion transporter (cMOAT) antisense cDNA enhances drug sensitivity in human hepatic cancer cells. Cancer Res 1997;57:5475–9.

[31] Zhou B. Gitschier J. hCTR1: a human gene for copper uptake identified by complementation in yeast. Proc Natl Acad Sci USA 1997;94:7481–6.

[32] Buchler M, Konig J, Brom M, Kartenbeck J, Spring H, Horie T, et al. cDNA cloning of the hepatocyte canalicular isoform of the multidrug resistance protein, cMrp, reveals a novel conjugate export pump deficient in hyperbilirubinemic mutant rats. J Biol Chem 1996; 271:15091–8.

[33] Petrukhin K, Lutsenko S, Chernov I, Ross BM, Kaplan JH, Gilliam TC. Characterization of the Wilson disease gene encoding a P-type copper transporting ATPase: genomic organization, alternative splicing, and structure/function predictions. Hum Mol Genet 1994;3: 1647–56.

[34] Grundemann D, Gorboulev V, Gambaryan S, Veyhl M, Koepsell H. Drug excretion mediated by a new prototype of polyspecific transporter. Nature 1994;372:549–52.

[35] Klein J, Bentur Y, Cheung D, Moselhy G, Koren G. Renal handling of cisplatin: interactions with organic anions and cations in the dog. Clin Invest Med 1991;14:388–94.

[36] Chirino YI, Hernandez-Pando R, Pedraza-Chaverri J. Peroxynitrite decomposition catalyst ameliorates renal damage and protein nitration in cisplatin-induced nephrotoxicity in rats. BMC Pharmacol 2004; 4:20.

[37] Jo SK, Cho WY, Sung SA, Kim HK, Won NH. MEK inhibitor, U0126, attenuates cisplatin-induced renal injury by decreasing inflammation and apoptosis. Kidney Int 2005;67:458–66.

[38] Kishore BK, Krane CM, Di Iulio D, Menon AG, Cacini W. Expression of renal aquaporins 1, 2, and 3 in a rat model of cisplatin-induced polyuria. Kidney Int 2004;58:701–11.

[39] Reece PA, Stafford I, Davy M, Freeman S. Disposition of unchanged cisplatin in patients with ovarian cancer. Clin Pharmacol Ther 1987;42:320–5.

[40] Urakami Y, Okuda M, Saito H, Inui K. Hormonal regulation of organic cation transporter OCT2 expression in rat kidney. FEBS Lett 2000; 473:73–6.

[41] Ji L, Masuda S, Saito H, Inui K. Down-regulation of rat organic cation transporter rOCT2 by 5/6 nephrectomy. Kidney Int 2002;62:514–524.

## Research Paper

# Pharmacokinetic Significance of Renal OAT3 (SLC22A8) for Anionic Drug Elimination in Patients with Mesangial Proliferative Glomerulonephritis

Yuji Sakurai,[1] Hideyuki Motohashi,[1] Ken Ogasawara,[1] Tomohiro Terada,[1] Satohiro Masuda,[1] Toshiya Katsura,[1] Noriko Mori,[2] Motokazu Matsuura,[3] Toshio Doi,[3] Atsushi Fukatsu,[4] and Ken-ichi Inui[1,5]

**Purpose.** Our previous studies showed that the mRNA level of human organic anion transporter (hOAT) 3 in the kidney was correlated with the rate of elimination of an anionic antibiotic cefazolin. However, the correlation coefficient was not so high. In the present study, therefore, we enrolled more patients to examine whether additional factors were responsible for the correlation.

**Methods.** hOAT mRNA levels in renal biopsy specimens were quantified using the real-time polymerase chain reaction method. The elimination rates for the free fraction of cefazolin were determined in patients with various renal diseases.

**Results.** In the present study, the coefficient of correlation between the hOAT3 mRNA level and the elimination rates for the free fraction of cefazolin was not so high in the patients overall as in our previous study ($r = 0.536$). However, following the classification of renal diseases, a better correlation was obtained in patients with mesangial proliferative glomerulonephritis ($r = 0.723$). In contrast, multiple regression analyses including gender, age, and liver function did not result in any improvements in the correlation coefficients.

**Conclusions.** These results suggest that the hOAT3 mRNA level is a significant marker of pharmacokinetics with which to predict the rate of elimination of cefazolin in patients with mesangial proliferative glomerulonephritis.

**KEY WORDS:** organic anion transporter; human kidney; renal diseases; real-time PCR; renal clearance.

## INTRODUCTION

In patients with renal impairment, individualized dosages are adjusted by using the plasma creatinine concentration or creatinine clearance ($C_{cr}$) to avoid adverse effects (1). $C_{cr}$ is often used to estimate the glomerular filtration rate (GFR), because creatinine is mainly eliminated via glomerular filtration. However, $C_{cr}$ would not reflect the true GFR, especially in patients with renal impairment, because the amount of tubular secretion is the negligible part of urinary excretion of creatinine (2). Recently, organic cation transporter (OCT) 2 (SLC22A2) was reported to transport creatinine suggesting that OCT2 plays an important role in the secretion of creatinine (3). Furthermore, accumulating

evidence shows a poor correlation between $C_{cr}$ and the urinary excretion of drugs (4,5), challenging the "intact nephron hypothesis" and suggesting that the renal handling of drugs may not decline in parallel. Therefore, it is necessary to identify more reliable markers to predict renal function such as the tubular secretion of drugs.

The renal handling of drugs involves three processes: glomerular filtration, tubular secretion, and reabsorption. Tubular secretion and reabsorption are mediated by various transporters expressed in the apical and basolateral membranes of the tubular epithelial cells (6,7). The organic anion transporters (OATs, SLC22A) can transport many ionic drugs and are expressed in the renal proximal tubules (8,9). However, the pharmacokinetic significance of each transporter in the clinical setting has not been fully elucidated.

Previously, we quantified the expression of hOAT1–4 mRNA and urinary excretion of the anionic antibiotic cefazolin in patients with renal diseases. The mRNA level of hOAT3, among the four anion transporters, significantly correlated with the rate of elimination of cefazolin ($n = 42$; $r = 0.44$, $p < 0.01$) (10). In addition, hOAT3 transported cefazolin. The renal expression level of hOAT3 possibly affects the renal handling of cefazolin. However, the coefficient of correlation between the hOAT3 mRNA level and elimination rate of cefazolin was not so high. Therefore, it is postulated that additional factors affect this coefficient.

[1] Department of Pharmacy, Kyoto University Hospital, Faculty of Medicine, Kyoto University, Sakyo-ku, Kyoto, Japan.
[2] Department of Nephrology, Shizuoka Prefectural Hospital, Shizuoka, Japan.
[3] Department of Clinical Biology and Medicine, Course of Biological Medicine, School of Medicine, University of Tokushima, Tokushima, Japan.
[4] Division of Artificial Kidneys, Kyoto University Hospital, Faculty of Medicine, Kyoto University, Kyoto, Japan.
[5] To whom correspondence should be addressed. (e-mail: inui@kuhp.kyoto-u.ac.jp)

**2016**

In our previous report, patients with various renal diseases were studied without classification. Because the cause and pathway of progression vary with the type of renal disease (11–13), proximal tubules may be exposed to different regulatory factors depending on the disease. In the present study, we enrolled more patients to examine whether the type of renal disease is a factor in the correlation between the hOAT3 mRNA level and the rate of elimination of cefazolin.

## MATERIALS AND METHODS

### Patients

A total of 75 patients were enrolled in the study (44 males and 31 females) aged 16–90 years (mean ± SD, 42.4 ± 18.5) with histopathologically confirmed renal disease. Patient profiles are described in Table I. Patients with mesangial proliferative GN ($n$ = 38; 22 males and 16 females, aged 39.8 ± 18.4 years), which is recognized as the most common form of primary renal disease, were categorized as Group I. Those with other renal diseases ($n$ = 37; 22 males and 15 females, aged 45.1 ± 18.5 years) were categorized into Group II. In Group II, eight patients had membranous nephropathy, eight had minimal change nephritic syndrome, seven had lupus nephritis, four had diabetic nephropathy, three had membranoproliferative GN, and seven had other renal diseases. Clinical tests, such as measurements of $C_{cr}$ or 120-min values of the phenolsulfonphthalein (PSP) test (PSP120′), were routinely conducted in the hospital to evaluate renal function. This study was conducted in accordance with the Declaration of Helsinki, and its amendments and was approved by the Kyoto University Graduate School and Faculty of Medicine, Ethics Committee. All patients gave written informed consent to participate in the study.

### Isolation of total RNA and genomic DNA

Total RNA from renal biopsy specimens and genomic DNA from blood in a guanidinium thiocyanate solution were isolated with a MagNA Pure LC RNA isolation Kit II and DNA isolation Kit I (Roche Diagnostic, Mannheim, Ger-

many), respectively. Total RNA was reverse-transcribed in the presence of RTmate solution (Wako Pure Chemical Industries, Osaka, Japan), and the single-stranded DNA was used for quantification of mRNA levels.

### Quantification of mRNA levels

The mRNA levels of hOAT1–4 were quantified as described previously (14). Using single-stranded DNA (ssDNA), a real-time polymerase chain reaction (PCR) was performed using the ABI Prism 7700 sequence detector (Applied Biosystems, Foster City, CA, USA). Reactions were carried out in duplicate under identical conditions. Glyceraldehyde-3-phosphate dehydrogenase (GAPDH) mRNA was also quantified as an internal control using GAPDH Control Reagent (Applied Biosystems).

### Measurement of Elimination Rate Constant for Free Fraction of Cefazolin

After renal biopsy, the patients received 1 g of cefazolin by intravenous infusion for 1 h as a prophylaxis of infection. Collection of blood samples and measurement of cefazolin concentrations by high-performance liquid chromatography (HPLC) were carried out as previously described (10). The plasma unbound fraction (fu) of cefazolin was determined by ultrafiltration using a micropartition system (MRS-1; Amicon, Inc., Beverly, MA, USA) (15). Free fraction of cefazolin was expressed as the ratio of the concentration in ultrafiltrate to that in plasma. The apparent elimination rate constant of the free fraction ($Ke_{free,cez}$) was calculated using the free fraction of the plasma cefazolin concentration immediately and 1 h after cefazolin infusion.

### Genotyping of the *hOAT3* gene

The genotypes of the *hOAT3* gene—C715T (Gln239Stop), T779G (Ile260Arg), C829T (Arg277Trp), A913T (Ile305Phe), C929T (Ala310Val), and G1342A (Val448Ile), which were reported in the public single nucleotide polymorphisms (SNPs) database NCBI dbSNP—were examined via the PCR restriction enzyme

**Table I.** Characteristics of Patients with Renal Disease

|                                      | All patients   | Group I       | Group II       | $p$ Value |
|--------------------------------------|----------------|---------------|----------------|-----------|
| No. of patients                      | 75             | 38            | 37             |           |
| Sex (males/females)                  | 44/31          | 22/16         | 22/15          |           |
| Age                                  | 42.4 ± 18.5    | 39.8 ± 18.4   | 45.1 ± 18.5    | 0.221     |
| Aspartate aminotransferase (IU/L)    | 19.6 ± 8.9     | 18.3 ± 6.9    | 20.9 ± 10.6    | 0.232     |
| Alanine aminotransferase (IU/L)      | 16.7 ± 10.1    | 14.9 ± 7.2    | 18.7 ± 12.2    | 0.113     |
| Lactate dehydrogenase (mg/L)         | 180.5 ± 52.8   | 171.3 ± 51.6  | 190.3 ± 53.1   | 0.139     |
| Serum creatinine (mg/dL)             | 1.1 ± 0.6      | 1.1 ± 0.7     | 1.0 ± 0.5      | 0.503     |
| Uric acid (mg/dL)                    | 6.3 ± 1.5      | 6.1 ± 1.4     | 6.4 ± 1.6      | 0.442     |
| Blood urea nitrogen (mg/dL)          | 17.6 ± 11.1    | 16.4 ± 8.0    | 18.8 ± 13.5    | 0.341     |
| Creatinine clearance (mL/min)        | 63.2 ± 28.1    | 64.6 ± 29.4   | 61.8 ± 27.0    | 0.672     |
| PSP120′ (%)                          | 64.9 ± 20.4    | 65.9 ± 18.7   | 63.4 ± 22.7    | 0.652     |
| $Ke_{free\ cez}$                     | 0.74 ± 0.25    | 0.73 ± 0.26   | 0.75 ± 0.25    | 0.619     |

Group I includes the patients with mesangial proliferative glomerulonephritis. All other patients were categorized in Group II.
Variance is indicated as the mean ± SD.
$p$ Values are for the comparison between Group I and Group II.